

AUG 22 2005

## REPORT DOCUMENTATION PAGE

Form Approved  
OMB No. 0704-0188

Public reporting burden for this collection of information is estimated to average 1 hour per response, including the time for reviewing instructions, searching existing data sources, gathering and maintaining the data needed, and completing and reviewing the collection of information. Send comments regarding this burden estimate or any other aspect of this collection of information, including suggestions for reducing this burden, to Washington Headquarters Services, Directorate for Information Operations and Reports, 1215 Jefferson Davis Highway, Suite 1204, Arlington, VA 22202-4302, and to the Office of Management and Budget, Paperwork Reduction Project (0704-0188), Washington, DC 20503.

1. AGENCY USE ONLY (Leave blank)		2. REPORT DATE 16.Aug.05	3. REPORT TYPE AND DATES COVERED MAJOR REPORT	
4. TITLE AND SUBTITLE AUTOMATIC LOW-VISIBILITY TRAJECTORY OPTIMIZATION FOR VISUALLY IDENTIFYING A SUSPECTED AIRCRAFT			5. FUNDING NUMBERS	
6. AUTHOR(S) 2D LT WHOLEY LEONARD N				
7. PERFORMING ORGANIZATION NAME(S) AND ADDRESS(ES) MASSACHUSETTS INSTITUTE OF TECHNOLOGY			8. PERFORMING ORGANIZATION REPORT NUMBER  CI04-1167	
9. SPONSORING/MONITORING AGENCY NAME(S) AND ADDRESS(ES) THE DEPARTMENT OF THE AIR FORCE AFIT/CIA, BLDG 125 2950 P STREET WPAFB OH 45433			10. SPONSORING/MONITORING AGENCY REPORT NUMBER	
11. SUPPLEMENTARY NOTES				
12a. DISTRIBUTION AVAILABILITY STATEMENT Unlimited distribution In Accordance With AFI 35-205/AFIT Sup 1			12b. DISTRIBUTION CODE <b>DISTRIBUTION STATEMENT A</b> Approved for Public Release Distribution Unlimited	
13. ABSTRACT (Maximum 200 words)				
14. SUBJECT TERMS			15. NUMBER OF PAGES 16	
			16. PRICE CODE	
17. SECURITY CLASSIFICATION OF REPORT	18. SECURITY CLASSIFICATION OF THIS PAGE	19. SECURITY CLASSIFICATION OF ABSTRACT	20. LIMITATION OF ABSTRACT	

AIAA Guidance, Navigation, and Control Conference and Exhibit, 15-18 August 2005, San Francisco, California

# Automatic Low-Visibility Trajectory Optimization for Visually Identifying a Suspected Aircraft

Leonard Wholey\* and Leena Singh†

*Massachusetts Institute of Technology, Cambridge, MA, 02139, USA*

This paper describes two methods used for producing trajectories, which enable an interceptor aircraft to perform a visual identification on a suspected aircraft. A trajectory typically used by fighter pilots is referred to as a beam intercept. The main goal for the maneuver is to put the interceptor in a relative position and heading with respect to the target such that it is in the best configuration to view the target aircraft's markings. Optimal trajectories complete this maneuver in minimum time and avoid detection. The first approach is formulated as a mixed integer linear programming problem which can be solved in real time. The linear cost function and constraints are adjusted to enable the interceptor to avoid radar detection. However, there are limitations to the accuracy of a radar detection model formed with only linear equations, which might justify using a nonlinear programming formulation. With this approach the interceptor's radar cross section and range between the suspected aircraft and interceptor can be incorporated into the problem formulation.

## I. Introduction

In recent air-to-air combat, many planes have been shot down in the beyond visual range region. During the Gulf war of 1991, this was the case in over 40% of the scenarios.<sup>9</sup> Improved radar and missile technology have decreased the chances of a dogfight. However, when a visual identification (VID) of an unidentified aircraft is necessary, a fighter pilot must be able to produce a trajectory, which enables a VID in minimum time while reducing the chances of being detected.

A frequently performed maneuver used for a VID is called a beam intercept.<sup>4</sup> As long as the target maintains an approximately constant heading, the maneuver can be performed with fairly low-g turns. This paper addresses some options for improving upon a fighter pilot's ability to perform an intercept on a single suspected aircraft. A computer could cue the pilot to an optimal trajectory which could decrease the amount of time required to complete the maneuver and reduce the chances of being detected by radar by managing range and attitude. Additionally, this scenario could be adapted to an unmanned aerial vehicle (UAV) equipped with a camera in order that a ground based operator could ultimately perform the VID.

Two methods were considered for calculating trajectories which model a beam intercept. The first method, which closely follows the approach in Richards,<sup>7</sup> is mixed integer linear programming (MILP). MILP is a powerful and effective method for solving rendezvous problems in real time.<sup>8</sup> The drawback of the approach for low-visibility trajectories is that it is difficult to accommodate certain nonlinear criteria, such as radar cross section, involved in producing a stealthy trajectory. As a result, we also formulate the problem as a nonlinear program using a direct trajectory optimization method sometimes referred to as direct collocation.<sup>3</sup> Although this allows a more accurate radar avoidance constraint, a real time solution is not guaranteed. A trajectory interpolation approach may be one solution to this problem, where a library of maneuvers parameterized by boundary conditions are stored offline; online, the automatic trajectory synthesis could interpolate to obtain a desired trajectory.<sup>2</sup>

\*Masters student, Department of Aeronautical and Astronautical Engineering, MIT; Charles Stark Draper Laboratory, 555 Technology Square, Cambridge, MA 02139, AIAA member

†Sr. Member Technical Staff, C.S. Draper Lab, 555 Technology Sq., Cambridge, MA. AIAA member

Copyright © 2005 by Leonard Wholey and Leena Singh. Published by the American Institute of Aeronautics and Astronautics, Inc. with permission.

20050831 061

The paper follows the following format. In section II, the details of the beam intercept maneuver are described. The aircraft radar detection model is explained in section III. For sections IV and V the MILP and direct collocation methods are outlined. In section VI, the results obtained from using both trajectory design methods are shown, and in section VII, conclusions and suggestions for future work are discussed.

## II. Beam Intercept Description

In order to visually identify the suspected aircraft, a fighter pilot will typically perform a maneuver called a beam intercept.<sup>1,4,6</sup> An example of this maneuver is shown in the figure below, where the interceptor, approaching from the right, is performing the maneuver on the target, on the left. Three regiments characterize this trajectory at the final state: (1) interceptor is a prescribed distance away from the target, (2) interceptor's velocity vector is pointed at the target, (3) angle between the line of sight vector and the target's velocity vector is between 90 and 110 degrees.<sup>1,6</sup> For the simulations presented in this paper, the desired angle is set to 90°.

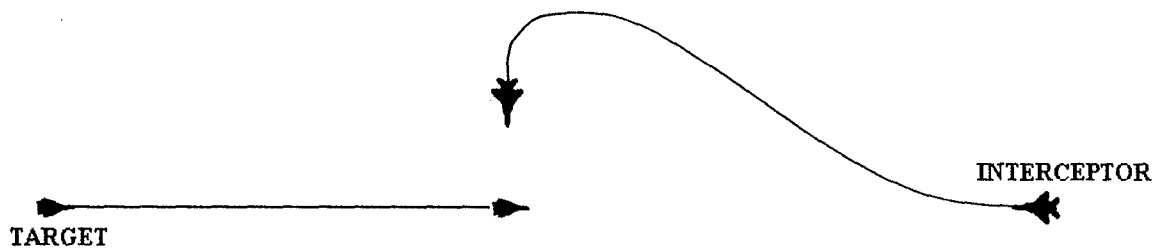


Figure 1. The above figure is a description of a beam intercept. The target has a constant speed and heading and is represented with the aircraft on the left. The interceptor is on the right and performs the beam intercept. This blind-side maneuver gives the interceptor a major tactical advantage over the target.

There are several advantages to performing a beam intercept as opposed to using proportional navigation, which might allow a faster merge:

- Decreases the chances of being detected by the target's radar
- Reduces the closing velocity which will allow more time for the VID, without this excess time the interceptor might have to reposition itself to obtain a firing opportunity
- Increases difficulty for the target to visually identify the interceptor, because during the final turn of the maneuver the interceptor is essentially pointed at the target
- Places the interceptor in an offensive position, in the event that the target is an enemy

In this research, we assume that the interceptor has perfect knowledge of the state of the target. This information could be provided by the aircraft's own radar or an Airborne Warning and Control System (AWACS) aircraft. Furthermore, we assume that the interceptor and target are at the same altitude. We introduce two different approaches for automatically synthesizing the trajectory.

## III. Radar Model

For an aircraft flying over a ground based radar, it is possible to significantly reduce the amount of time during which the aircraft may be detected.<sup>5</sup> The same should be true in performing a beam intercept with a possibility of avoiding radar detection completely.

In order to avoid radar detection, the interceptor can affect three variables. The maximum half cone angle for aircraft radar typically ranges between 45 to 60 degrees. As a result the interceptor can fly a significant portion of the trajectory outside of the radar cone where radar detection is impossible. Within the cone, the power received by radar is inversely proportional to range  $R$  and directly proportional to radar cross section  $\sigma$

$$P \propto \frac{\sigma}{R^4} \quad (1)$$

In performing a beam intercept, the interceptor must maintain a large distance between itself and the target until it has flown outside of the target's radar cone. Additionally, the interceptor can also affect its radar cross section, which is a function of the interceptor's azimuth  $\kappa_r$  and elevation  $\theta_r$  angles relative to the target aircraft. These angles are determined with the equations<sup>5</sup>

$$\hat{x}_b = R_{be}\hat{x}_e \quad (2)$$

$$\kappa_r = \arctan\left(\frac{-\hat{x}_{b,2}}{\hat{x}_{b,1}}\right) \quad (3)$$

$$\theta_r = \arctan\left(\frac{-\hat{x}_{b,3}}{\sqrt{\hat{x}_{b,1}^2 + \hat{x}_{b,2}^2}}\right) \quad (4)$$

where  $R_{be}$  is a rotational matrix which rotates the unit relative position vector between the target and the interceptor,  $\hat{x}_e$ , from an earth frame to a body frame,  $\hat{x}_b$ .  $\hat{x}_b$  is a three dimensional vector where  $\hat{x}_{b,i}$  represents the  $i^{th}$  component of  $\hat{x}_b$ . For the direct collocation development described in section V, a generic aircraft radar cross section model is used similar to the one found in Norsell,<sup>5</sup> where a bivariate cubic spline is used to map the interceptor's azimuth and elevation angles to  $\sigma$ , as shown in Figure 2.

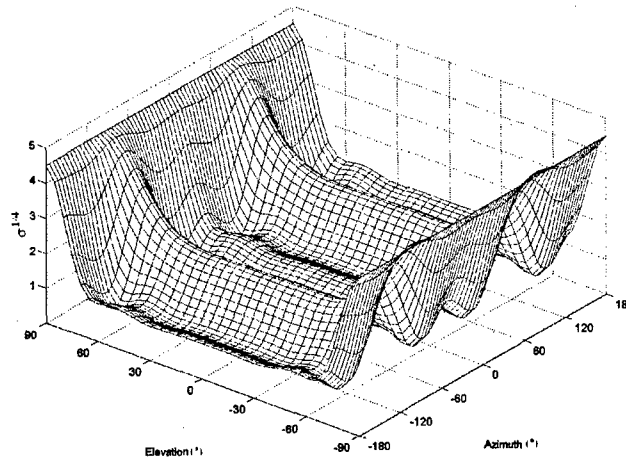


Figure 2. Generic Aircraft Radar Cross Section Model<sup>5</sup>

#### IV. MILP Approach

MILP is an optimization based approach which can be used to solve an optimal control problem in real time. The problem is discretized with  $N$  nodes, where linear equations describe the vehicle's state at each node. Constraints on the vehicle's states and controls can be added as long as they occur in linear form, and adjoint binary variables are used in order to impose or relax relevant constraints.

This approach closely follows the method presented in Richards<sup>7</sup> with variations in the cost function and constraints. Richards has shown that MILP can be used in real time for a rendezvous between two vehicles.<sup>8</sup> This problem is very similar to the beam intercept, wherein the interceptor essentially performs a rendezvous with an offset distance along with the other requisites described in section II.

While the rendezvous problem<sup>8</sup> models the dynamics in the relative frame, the dynamics for this approach include only the interceptor's states. We project the target aircraft's position and velocity to produce its baseline trajectory. Solving for the controls,  $f_{x,k}$  and  $f_{y,k}$  which are the interceptor's forces in the inertial  $x$  and  $y$  direction at time step  $k$ , will produce the desired trajectory according to the following dynamics and constraints. Using a set of  $N$  nodes, the dynamics of the aircraft are discretized with the linear equations

$$\ddot{x}_{int,k} = \frac{f_{x,k}}{mass} \quad (5)$$

$$\ddot{y}_{int,k} = \frac{f_{y,k}}{mass} \quad (6)$$

$$\forall k \in [1 \dots N - 1]$$

where  $(x_{int,k}, y_{int,k})$  are the interceptor's  $x$  and  $y$  position in the inertial frame. Similarly  $(\dot{x}_{int}, \dot{y}_{int})$  and  $(\ddot{x}_{int}, \ddot{y}_{int})$  are the interceptor's velocities and accelerations in the inertial frame. The time between each node is defined as  $\Delta t(k)$ . The maximum speed  $v_{max}$  and maximum force  $f_{max}$  at each node are approximated with the linear constraints

$$\dot{x}_{int,k} \sin \frac{2\pi m}{M} + \dot{y}_{int,k} \cos \frac{2\pi m}{M} \leq v_{max} \cos \frac{\pi}{M} \quad (7)$$

$$\forall k \in [1 \dots N], m \in [1 \dots M]$$

$$f_{x,k} \sin \frac{2\pi m}{M} + f_{y,k} \cos \frac{2\pi m}{M} \leq f_{max} \cos \frac{\pi}{M} \quad (8)$$

$$\forall k \in [1 \dots N - 1], m \in [1 \dots M]$$

where  $M$  is the number of linear constraints used to approximate a 2 norm. With larger values of  $M$ , the set of constraints approaches an actual magnitude constraint of the velocity and force vectors.

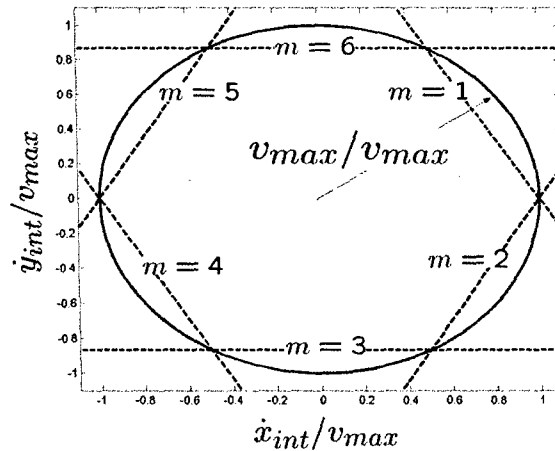


**Figure 3.** Linear constraints are used to approximate the maximum speed limit  $v_{max}$ . The lines  $m = 1 \dots 6$  represent each of the linear inequalities.

A limit on minimum speed is not included in the problem formulation. This can result in infeasible trajectories, where the solution produced by the optimizer might exceed a maximum turn rate given the speed of the aircraft, or the aircraft might stall. A minimum speed constraint with the same accuracy as the maximum speed approximation would require  $N \times M$  binary variables. This slowed the run time of the MILP optimization software Xpress<sup>10</sup> significantly. Otherwise, the turn rate constraint can also be satisfied by decreasing  $f_{max}$ .<sup>7</sup>

The interceptor's desired endstate changes in order to include a maneuvering target, whose position and velocity at each node  $k$  are specified before the MILP step

$$x_{des,k} = x_{tgt,k} + R_s \cos(\Psi_{tgt,k} \pm 90^\circ) \quad (9)$$

$$y_{des,k} = y_{tgt,k} + R_s \sin(\Psi_{tgt,k} \pm 90^\circ) \quad (10)$$

$$\dot{x}_{des,k} = \frac{\dot{x}_{tgt,k} \cos(\mp 90^\circ) - \dot{y}_{tgt,k} \sin(\mp 90^\circ)}{\sqrt{\dot{x}_{tgt,k}^2 + \dot{y}_{tgt,k}^2}} v_s \quad (11)$$

$$\dot{y}_{des,k} = \frac{\dot{x}_{tgt,k} \sin(\mp 90^\circ) + \dot{y}_{tgt,k} \cos(\mp 90^\circ)}{\sqrt{\dot{x}_{tgt,k}^2 + \dot{y}_{tgt,k}^2}} v_s \quad (12)$$

$$\forall k \in [1 \dots N]$$

where  $(x_{des,k}, y_{des,k})$  are the desired interceptor  $x$  and  $y$  position.  $(\dot{x}_{des,k}, \dot{y}_{des,k})$  are the desired interceptor  $x$  and  $y$  velocity.  $(x_{tgt}, y_{tgt})$  and  $(\dot{x}_{tgt}, \dot{y}_{tgt})$  are the target's  $x$  and  $y$  position and  $x$  and  $y$  velocity respectively.  $\Psi_{tgt,k}$  is the target's heading, and  $R_s$  is the desired range between the target and the interceptor once the beam intercept is completed. At the end of the engagement, the interceptor is also required to have a heading  $\pm 90^\circ$  relative to the target. MILP software could be used to solve both problems with additional binary variables, or a heuristic could be applied which defines in general when one heading should be applied over the other.

The following binary constraints model the completion of the beam intercept

$$X_{int} - X_{des} \leq Hw_k \quad (13)$$

$$-X_{int} + X_{des} \leq Hw_k \quad (14)$$

$$\forall k \in [1 \dots N]$$

where  $X_{int}$  represents the set of variables  $(x_{int,k}, y_{int,k})$ ,  $(\dot{x}_{int,k}, \dot{y}_{int,k})$  and  $X_{des}$  represents  $(x_{des,k}, y_{des,k})$ ,  $(\dot{x}_{des,k}, \dot{y}_{des,k})$ .  $H$  is a large positive number, and  $w_k$  is a binary variable which allows the constraints to be relaxed. This formulation admits solutions that drive the interceptor to intersect the candidate set of desired interceptor states produced earlier. If the interceptor has reached the candidate relative position and velocity at node  $k$ , then  $w_k = 0$  which is shown in Figure 4.

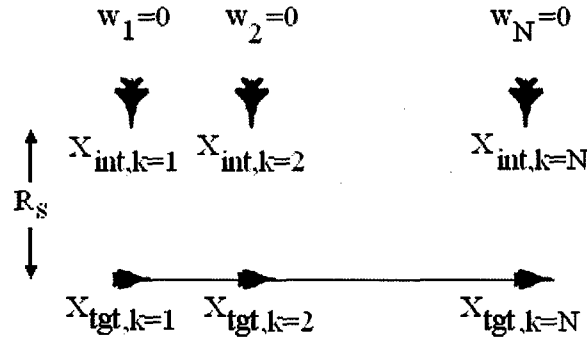


Figure 4. This figure shows the candidate endstates of the interceptor at each node  $k$  for a target with a constant heading.  $X_{int,k}$  and  $X_{tgt,k}$  contain the states of the interceptor and target respectively, and  $R_s$  is the desired separation distance. If there is a feasible solution at an endstate, the binary variable  $w_k$  can be set to zero, otherwise it is set to one in order to relax the desired endstate constraint. MILP solves multiple linear programming problems where the binary variables  $w_k$  are varied in order to find a feasible, optimal solution.

This relaxation of the constraints is represented in the objective function as the variable  $t_k$ . At node  $k$  if  $w_k = 0$ , then  $t_{k \dots N} = 0$  otherwise  $t_k = 1$ . In order to enforce that the maneuver is completed at some time step  $k$ , an additional constraint is added

$$\sum_{k=1}^N t_k \leq N - 1 \quad (15)$$

The objective is to minimize the time to complete the beam intercept and the accelerations over the course of the mission. In order to approximate our objective of maximizing the range between the two aircraft within the linear cost formulation structure that MILP permits, we introduce the term  $c|y_k|$

$$\min_{f_{x,k}, f_{y,k}} J = \sum_{k=1}^N (\epsilon|f_{x,k}| + \epsilon|f_{y,k}| + t_k - c|y_k|) \quad (16)$$

Through  $c|y_k|$ , the interceptor is encouraged to maximize its  $y$  distance relative to the target throughout the trajectory. This formulation allows us to approximately penalize proximity with the target. The target's initial position is placed at the origin with its velocity vector pointed along the x-axis, so that with larger values of  $c$  the interceptor will maintain higher values of range throughout the trajectory. This could potentially decrease the chances of being detected by the target's radar because the amount of power that the aircraft's radar receives is heavily dependent on range.

In the results section, the problem is solved once during the maneuver, given the initial states of the interceptor and the target's projected trajectory. However, the problem could be resolved if the target deviates significantly from its previously calculated path.

### A. Additional State Constraint for Radar Detection Avoidance

Another method for avoiding radar detection involves breaking up the trajectory planning problem into two segments. The first segment entails the interceptor flying to a point of at least a certain distance  $RR$  along the target's radar cone. If the value for  $RR$  is sufficiently large given the radar cross section of the interceptor and the efficacy of the target's radar, then it is reasonable to assume that the interceptor will not be detected by radar. Beyond this point then, we continue the solution with a range independent formulation for the intercept problem. This method has the advantage over the previous approach in that the interceptor only maintains distance from the target while within the target's radar cone.

This method uses the equations as previously described but with an additional requirement that the interceptor is required to fly to two waypoints. The  $c|y_k|$  term is also removed from the cost function. The first point, described in Figure 5, is a distance of at least a certain range  $RR$  along the target's radar cone

$$(x_{int,k} - x_{tgt,k}) - RR \cos(RCA + \Psi_{tgt,k}) \leq H v_k \quad (17)$$

$$-(x_{int,k} - x_{tgt,k}) + RR \cos(RCA + \Psi_{tgt,k}) \leq H v_k \quad (18)$$

$$-(y_{int,k} - y_{tgt,k}) + RR \sin(RCA + \Psi_{tgt,k}) \leq H v_k \quad (19)$$

$$\forall k \in [1 \dots N]$$

where  $RCA$  is the radar cone angle limit and  $v_k$  is a binary variable. Now,  $t_{k \dots N} = 0$  if both  $v$  and  $w$  are zero at previous time steps. The second point is the previously defined completion state of the maneuver.

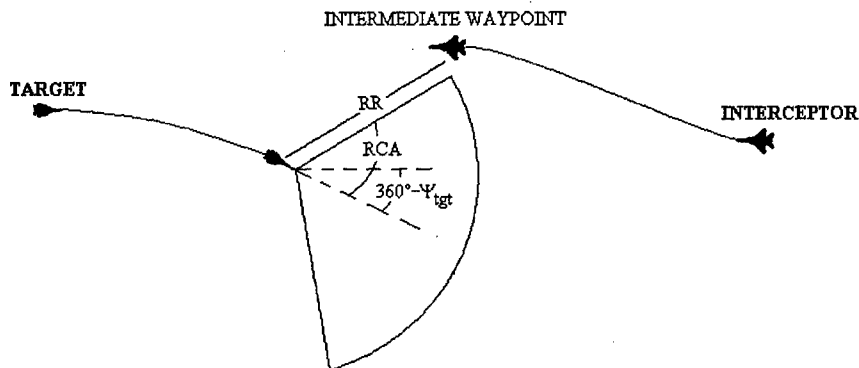


Figure 5. In order to reduce the chances of being detected by the target's radar, the MILP problem is formulated with an additional constraint that the interceptor is required to fly to an intermediate waypoint of at least a distance  $RR$  along the radar cone.  $RCA$  indicates the maximum angle at which the target's radar will function, and  $\Psi_{tgt}$  is the target's heading.

## V. Direct Collocation Approach

While the MILP approach can create feasible trajectories for a beam intercept in real time, it is difficult to formulate a linear constraint that models the radar cross section of an aircraft. The following direct collocation approach can address this issue, although the nonlinear programming formulation might result in longer computation times without a guarantee of converging to a feasible solution.

With direct collocation, the states are approximated with cubic polynomials and the controls are found by linearly interpolating between nodes.<sup>3</sup> The dynamics are discretized with  $N$  nodes using collocation of the states and controls. Now, the dynamics are approximated with algebraic equations, and the problem is formulated as a nonlinear program. Solutions for this paper are produced using the function `fmincon` in MATLAB's Optimization Toolbox.

We use a lateral aircraft model for this method assuming a constant speed for the interceptor and a constant speed and turn rate for the target. Also, the interceptor and target are flying at the same altitude. The model dynamics are described in a relative frame with the following equations

$$\dot{x}_{rel} = v_{int} \cos(\Psi_{int}) - v_{tgt} \cos(\Psi_{tgt}) \quad (20)$$

$$\dot{y}_{rel} = v_{int} \sin(\Psi_{int}) - v_{tgt} \sin(\Psi_{tgt}) \quad (21)$$

$$\dot{\Psi}_{int} = \frac{\tan(\phi)g}{v_{int}} \quad (22)$$

$$\dot{\Psi}_{tgt} = d \quad (23)$$

where  $x_{rel}$  and  $y_{rel}$  are the  $x$  and  $y$  position of the interceptor with respect to the target,  $v_{int}$  and  $v_{tgt}$  are the interceptor and target speed respectively,  $\phi$  is the interceptor's bank angle,  $\Psi_{int}$  and  $\Psi_{tgt}$  are the interceptor and target heading respectively, and  $d$  is the target's turn rate.

The problem is formulated as a nonlinear program where the states include the following values:  $x_{rel}(k)$ ,  $y_{rel}(k)$ , and  $\Psi_{int}(k)$ , and the control is  $\phi(k)$  where  $\forall k \in [1 \dots N]$ . There is also a variable for final time  $t_f$ , and the nodes are equally spaced in time. The objective is to perform the maneuver in minimum time with control weighting to assist in covering to a locally optimal, feasible solution

$$\min_{\phi(k)} J = t_f + p \sum_{k=1}^N \phi^2(k) \quad (24)$$

where  $p$  is a small constant.

The constraints for the NLP include dynamic feasibility which is approximated using collocation.  $\Delta_{k,j}$  represent the dynamics of equations (20-22), whereas equation (23) is easily integrated to find the target's heading at each node. The constraints also include a limit on the maximum bank angle, radar detection avoidance, and final desired heading and position

$$\Delta_{k,j} = 0 \quad (25)$$

$$\forall k \in [1 \dots N], \forall j \in [1 \dots m]$$

$$\phi_{min} \leq \phi(k) \leq \phi_{max} \quad (26)$$

$$R_d(k) \leq \sqrt{x_{rel}^2(k) + y_{rel}^2(k)} \quad (27)$$

$$\Psi_{tgt}(N) - \Psi(N) = 90^\circ \quad (28)$$

$$x_{rel}(N) = R_s \cos(\Psi_{tgt}(N) + 90^\circ) \quad (29)$$

$$y_{rel}(N) = R_s \sin(\Psi_{tgt}(N) + 90^\circ) \quad (30)$$

where  $R_d(k)$  is the range at which the target's radar can detect the interceptor at node  $k$ , and  $R_s$  is the final separation range to complete the beam intercept.  $R_d(k)$  is defined as

$$R_d(k) = \frac{\nu \sigma^{\frac{1}{4}}(k)}{1 + e^{-\alpha \zeta(k)}} \quad (31)$$

$$\zeta(k) = \begin{aligned} &\cos(90^\circ - (RCA + \Psi_{tgt}(k)))x_{rel}(k) - \\ &\sin(90^\circ - (RCA + \Psi_{tgt}(k)))y_{rel}(k) \end{aligned} \quad (32)$$

where  $\nu$  is a variable dependent on the power of the target's radar,  $\sigma(k)$  the interceptor's radar cross section,  $a$  a constant which is explained later,  $\zeta(k)$  the distance from the radar cone (shown in Figure 6), and  $RCA$  the radar cone angle.

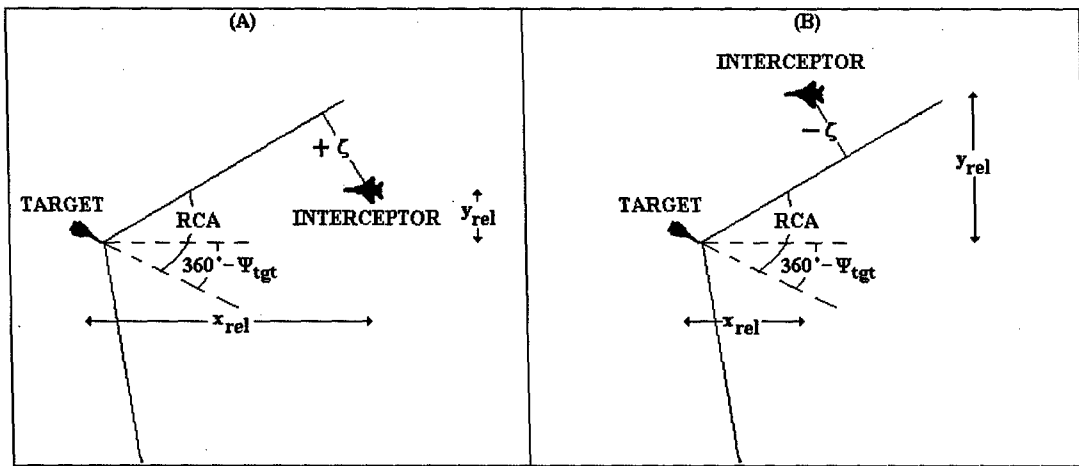


Figure 6.  $\zeta$  is the distance from the interceptor to the edge of the target's radar cone and is defined as positive (Figure A) if the interceptor is within the region of detection and negative otherwise (Figure B).  $RCA$  is the target's radar cone angle, and  $\psi_{tgt}$  is the target's heading.

For this scenario,  $\sigma(k)$  is a function of  $\phi(k)$ ,  $\psi_{int}(k)$ ,  $x_{rel}(k)$ , and  $y_{rel}(k)$  where the function of these variables is described in section III. It is assumed that the interceptor's angle of attack is nearly a constant throughout the trajectory and does not significantly change the radar cross section of the aircraft.

With the detection range constraint, the sigmoid form of equation (31) allows the aircraft to fly outside of the radar cone without concern for radar cross section or range. For this simulation,  $a = 16.39/km$  so that if  $\sigma = 1m^2$ , then the radar detection range can be described with the curves in Figure 7 where  $R_d$  varies according to the strength of the target's radar.

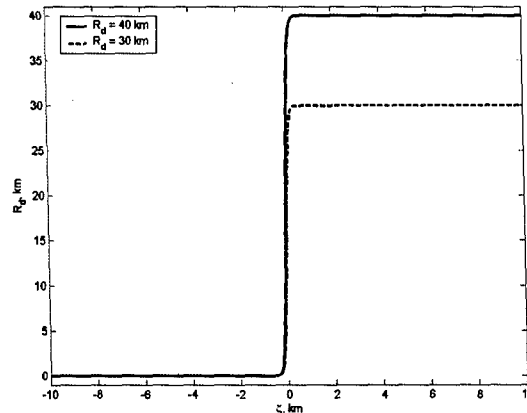


Figure 7. Radar detection range as a function of distance from the radar cone  $\zeta$  with radar cross section held constant

With larger values of  $a$ , the radar constraint becomes more like a binary switch. However, if this value was set too large, then the optimization software had difficulties in converging to an answer.

## VI. Results

For the following the simulations, initially the target and interceptor are heading towards each other and are separated by 27.5km. The two aircraft have the same initial speed, and the target is turning to the right with a constant turn rate. Three different methods are applied to solve the beam intercept problem. The first involves using MILP to calculate a trajectory where the objective includes maintaining a larger distance from the target throughout the maneuver. The second approach also uses MILP with an additional requirement that the interceptor is required to fly to a point of at least a certain distance along the target's radar cone edge. The final approach uses direct collocation which allows a higher fidelity radar cross section model of the interceptor.

### A. MILP Results with Adjusted Cost Function

As presented in section IV, the cost function for the beam intercept scenario is

$$\min_{f_{x,k}, f_{y,k}} J = \sum_{k=1}^N (\epsilon |f_{x,k}| + \epsilon |f_{y,k}| + t_k - c |y_k|) \quad (33)$$

where the  $c|y_k|$  term encourages the interceptor to maintain a standoff range from the target vehicle. The constants for the MILP simulations are

Table 1. Constants for MILP beam intercept simulations

$N$	60	$M$	10
$mass$	10,442kg	$H$	100,000
$v_{max}$	167m/s	$f_{max}$	313kN
$x_{int,k=1}$	27.5km	$y_{int,k=1}$	0km
$x_{tgt,k=1}$	0km	$y_{tgt,k=1}$	0km
$\dot{x}_{int,k=1}$	-152.5m/s	$\dot{y}_{int,k=1}$	0m/s
$\dot{x}_{tgt,k=1}$	152.5m/s	$\dot{y}_{tgt,k=1}$	0m/s
$v_s$	152.5m/s	$R_s$	3.05km
$\epsilon$	$1 \times 10^{-9}$	$\Delta t(k)$	2s

The first results show solutions to the problem with variations on the weighting factor  $c$  of  $c|y_k|$ . Using a 1.50 GHz desktop with 1.00 GB of RAM, Xpress software is typically able to solve this problem in 2-6 seconds, as shown in Table 2.

Table 2. Results from MILP beam intercept trajectories including  $c|y_k|$  term in cost function

	path length (km)	trajectory time (s)	computation time (s)	active $f_x, f_y$ duration (s)	min/max speed (m/s)
$c = 0$	14.2	88	2.9	26	150/159
$c = 10 \cdot 10^{-6}$	14.7	88	4.7	48	153/167
$c = 20 \cdot 10^{-6}$	15.0	90	5.2	50	153/167
$c = 50 \cdot 10^{-6}$	17.8	108	5.3	74	150/167
$c = 100 \cdot 10^{-3}$	18.2	118	3.4	68	106/167

Figures 8 and 9 show two examples of a beam intercept and the corresponding control histories. With the largest value of the  $y$  weighting coefficient, the maneuver requires significantly more control effort and the time to completion is 30 seconds longer than the shortest trajectory, as shown in Table 2. In both scenarios, at the end of the maneuver the interceptor has a 3.05km separation distance from the target and a terminal heading  $90^\circ$  different than target's.

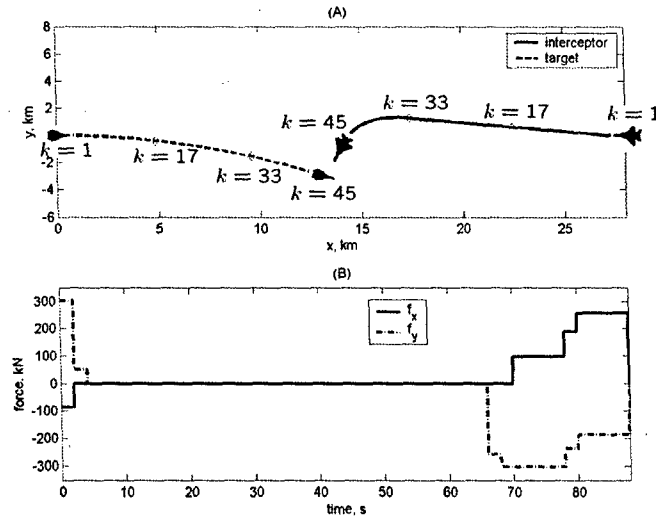


Figure 8. Beam intercept using MILP with  $y$  weighting coefficient  $c = 0$ . Figure (A) shows the interceptor and target trajectory, and Figure (B) shows the interceptor's controls during the maneuver. The target is turning at a constant rate of  $0.3^\circ/s$ . A large control action is required at the beginning of the trajectory in order to change the heading of the interceptor. For the majority of the maneuver, the interceptor maintains this heading, and then finally a large control effort is applied in order to obtain the desired relative heading and position.

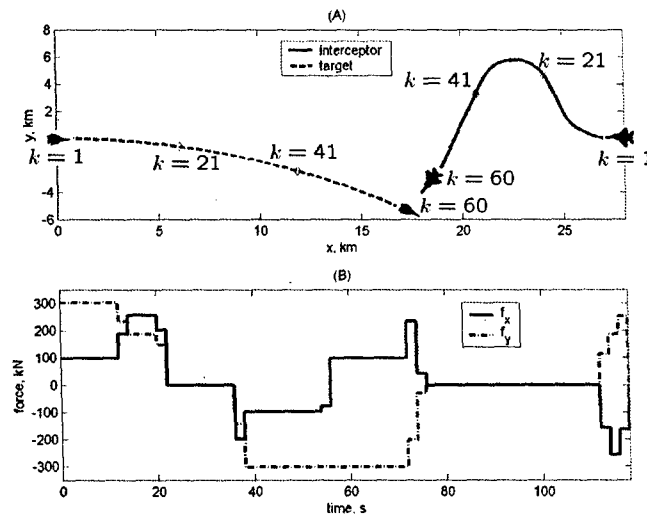


Figure 9. Beam intercept using MILP with  $y$  weighting coefficient  $c = 0.1$  which encourages the interceptor to increase its cross-range from the target. Figure (A) shows the interceptor and target trajectory, and Figure (B) shows the interceptor's controls during the maneuver. The target is turning at a constant rate of  $0.3^\circ/s$ . Initially, the interceptor makes a sharp turn to the right in order to obtain a larger distance from the target. Then, the interceptor briefly travels along a straight path and banks left to head towards the target. After following along another straight path, a small turn is applied to complete the maneuver.

Figure 10 shows how the  $c|y_k|$  term influences the range between the interceptor and target during the beam intercept. The four curves are from the trajectories in Table 2.

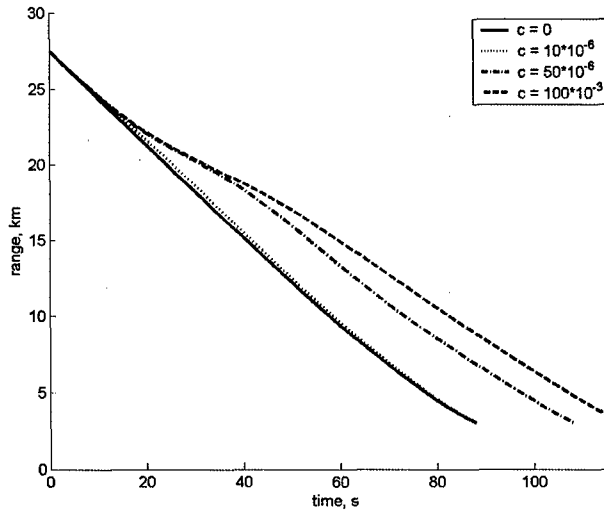


Figure 10. With higher values of the constant  $c$ , the interceptor maintains a larger distance from the target throughout the trajectory.

A range of trajectories can be created by varying  $c$ . However, there is no guarantee that the interceptor will avoid radar detection. After the trajectory is created, one could include a separate evaluation to determine if the interceptor would be detected by the target's radar. If the trajectory fails the test, the algorithm could run iteratively with larger values of  $c$ .

### B. MILP Results with Additional State Constraint for Radar Detection Avoidance

For this formulation, the interceptor is required to fly to a point of at least a certain distance  $RR$  along the radar cone where the radar cone angle  $RCA$  is limited to  $45^\circ$ . The cost function for this scenario is

$$\min_{f_{x,k}, f_{y,k}} J = \sum_{k=1}^N (\epsilon|f_{x,k}| + \epsilon|f_{y,k}| + t_k) \quad (34)$$

so that now the interceptor must fly to both waypoints in minimum time with a small weight on control effort. With the additional binary variables required for this approach, the computation times are significantly longer as seen by comparing the results in Table 3 to the results without the constraint in Table 2.

In Figures 11 and 12, the interceptor flies to a point of exactly the required distance along the radar cone and finishes the trajectory with the desired relative heading of  $90^\circ$  and range of  $3.05\text{km}$ .

Table 3. Results from MILP beam intercept trajectories including a constraint to fly to point of at least a distance  $RR$  along the radar cone edge

	path length (km)	trajectory time (s)	computation time (s)	active $f_x, f_y$ duration (s)	min/max speed (m/s)
$RR = 9.2\text{km}$	14.5	90	10.1	32	151/163
$RR = 12.2\text{km}$	16.2	102	29.9	48	124/165

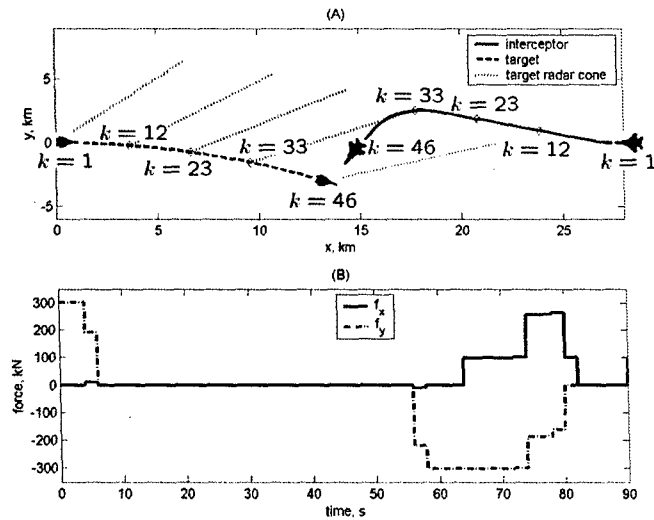


Figure 11. Beam intercept using MILP where interceptor is required to fly to a distance of at least  $9.2\text{km}$  along the target's radar cone. Figure (A) shows the aircrafts' trajectories along with the radar cone limit of the target, and Figure (B) is the interceptor's control history. The target is turning at a constant rate of  $0.3^\circ/\text{s}$ . The interceptor begins the maneuver with a right turn in order reach the end of the target's radar cone. Shortly before reaching this point, a hard left turn is executed to wrap around the radar cone and to point the interceptor towards the desired endstate.

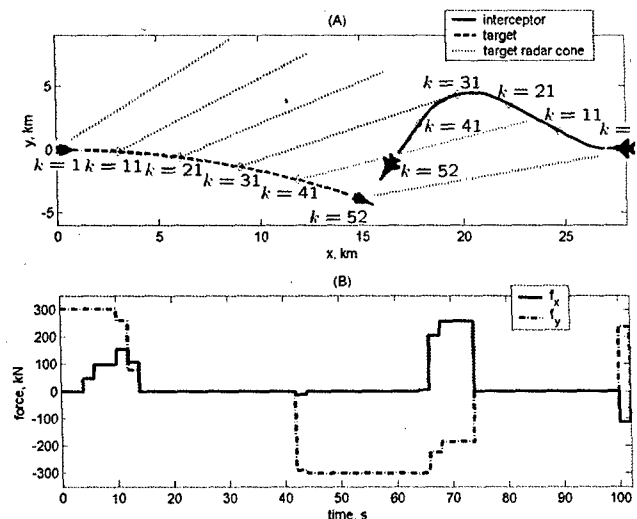


Figure 12. Beam intercept using MILP where interceptor is required to fly to a distance of at least  $12.2\text{km}$  along the target's radar cone. Figure (A) shows the aircrafts' trajectories along with the radar cone limit of the target, and Figure (B) is the interceptor's control history. The target is turning at a constant rate of  $0.3^\circ/\text{s}$ . The interceptor performs the maneuver in a similar manner as Figure 11 but with exaggerated turns in order to fly around the stronger radar.

### C. Direct Collocation with Radar Avoidance Constraints Results

For the following scenarios, the interceptor and target maintain a constant speed and altitude. The interceptor's objective is to complete the maneuver in minimum time with a small weight on bank angle

$$\min_{\phi(k)} J = t_f + p \sum_{k=1}^N \phi^2(k) \quad (35)$$

Additionally, the interceptor must avoid radar detection throughout the trajectory. Table 4 shows the constants used for the first two simulations. In Figure 13, a trajectory is shown where the interceptor ignores the radar of the target, and in Figure 14 radar constraints are added with the target's radar detection range set to 12.2km when the interceptor's radar cross section is 1m<sup>2</sup>. In exchange for attempting to avoid radar detection, the trajectory duration is 11.6 seconds longer.

Table 4. Constants for direct collocation simulations with constant speed aircraft model

$N$	50	$g$	9.8m/s <sup>2</sup>
$\phi_{min}$	-60°	$\phi_{max}$	60°
$\Psi(t_0)$	180°	$\Psi_{tgt}(t_0)$	0°
$v$	152.5m/s	$v_{tgt}$	152.5m/s
$x_{rel}(t_0)$	27.5km	$y_{rel}(t_0)$	0km
$R_s$	3.05km	$RCA$	45°
$p$	0.1		

Table 5. Results for constant speed trajectories including radar avoidance constraints. The term  $R_d(\sigma = 1m^2)$  refers to the detection range of the target's radar when the interceptor's radar cross section is 1m<sup>2</sup>.

	path length (km)	trajectory time (s)	computation time (s)
$R_d(\sigma = 1m^2) = 0km$	13.6	89.1	15.1
$R_d(\sigma = 1m^2) = 12.2km$	15.4	100.7	52.6

Because the detection range constraint is only applied at the nodes, for nearly every simulation the interceptor is detected by the target's radar for a brief moment before crossing the radar cone as shown in Figure 15. There are a few variations to the formulation which might prevent this problem. The density of the nodes around this area could be increased, using the previously calculated trajectory as an initial guess in forming a new solution. Also, the optimization problem could be solved increasing the target's radar power to more than its actual value. Finally, the sigmoid equation could be altered with the term  $b$  in order to shift the radar cone

$$\frac{v\sigma^{\frac{1}{4}}(k)}{1 + e^{-a\zeta(k)}} \Rightarrow \frac{v\sigma^{\frac{1}{4}}(k)}{1 + e^{-a(\zeta(k)+b)}} \quad (36)$$

A problem with casting the optimal control problem as a nonlinear program is the existence of multiple local minima. Of 1,140 simulations run using MATLAB's Optimization Toolbox, which varied with initial position of the interceptor with respect to the target and target radar strength, 99.74% appear to be solutions that could be globally optimal. For the three cases which were clearly local minima, the simulation was performed again, changing the guess of the initial variables at the nodes by multiplying by 1.1, and a better solution was obtained. One example is shown in Figure 16.

Another issue with nonlinear programming is the time duration for the optimization software to converge to a solution. Of the 1,140 simulations, the average computation time to reach a locally optimal solution was 24.25 seconds with a standard deviation of 19.04 seconds. In compiled implementation and on a faster processor, these computation times may be acceptable for real-time implementation. However, the maximum

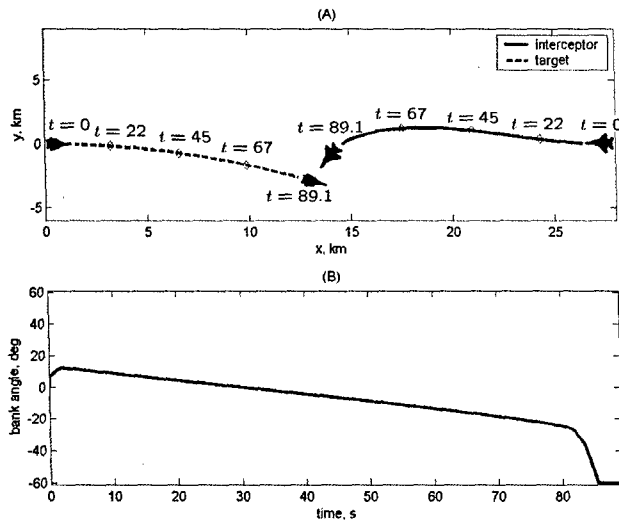


Figure 13. For this scenario, the detection range of the target's radar is set to zero,  $R_d(\sigma = 1m^2) = 0km$ , and the target is turning at a constant rate of  $0.3^\circ/s$ . Figure (A) shows the trajectories of both aircraft, and Figure (B) is the bank angle history of the interceptor. The interceptor initially makes a small turn away from the target followed by a very gradual turn towards the target. At the end of the trajectory, a sharp turn is applied to achieve the final desired relative heading and position.

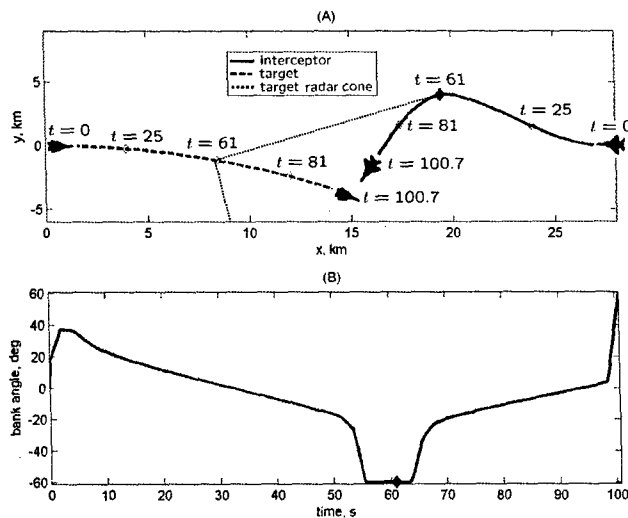


Figure 14. In this case, the detection range of the target's radar is  $12.2km$  when the interceptor presents a radar cross section of  $1m^2$ , and the target is turning at a constant rate of  $0.3^\circ/s$ . Figure (A) shows the trajectories of the aircraft, and Figure (B) is the bank angle history of the interceptor. The interceptor begins the maneuver with a turn away from the target to fly to the point, shown with a solid black diamond, at which it will cross the target's radar cone. Just before reaching this point, maximum negative bank angle is applied to return the interceptor to a heading which will allow completion of the maneuver. The interceptor travels along a nearly straight path and then finally applies maximum positive bank angle to obtain the desired endstate.

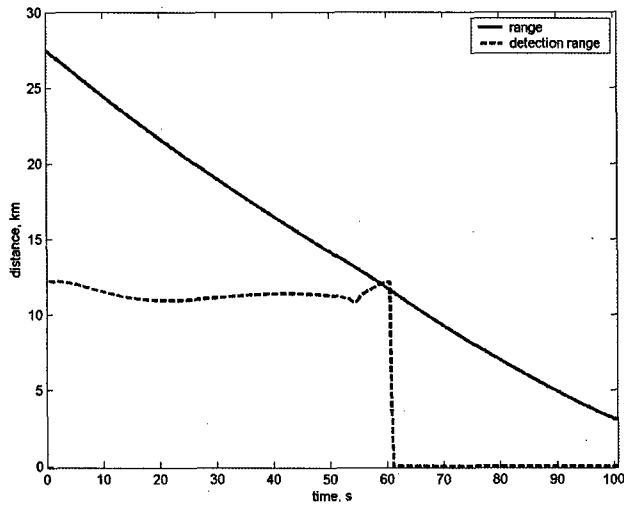


Figure 15. Limitation of radar avoidance constraint for the simulation where  $R_d(\sigma = 1m^2) = 12.2km$ . The interceptor is detected by the target's radar for a brief moment just before crossing the target's radar cone.

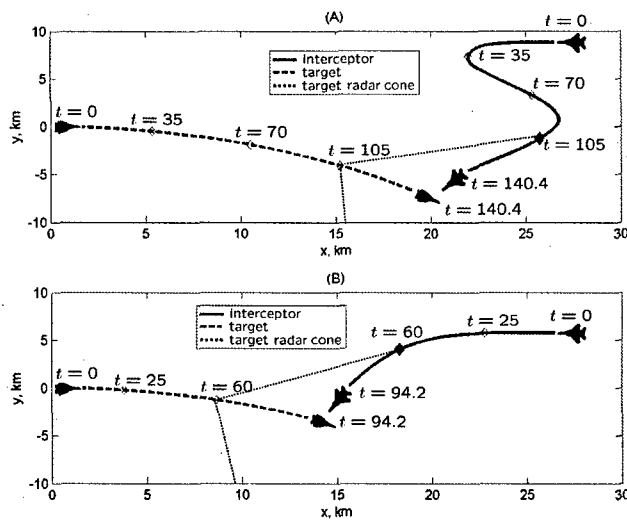


Figure 16. This figure shows two locally optimal trajectories where each was produced using a different initial guess for the NLP variables. Trajectories (A) and (B) are completed in 140.4s and 94.2s respectively. The solid black diamond is the point at which the interceptor crosses the target's radar cone.

computation time was over 6 minutes. This uncertainty in reaching a locally optimal solution clearly makes online implementation difficult.

## VII. Conclusion

Two approaches have been shown to produce feasible trajectories that resemble the fighter pilot maneuver called a beam intercept. While the first MILP formulation is able to produce a trajectory in a few seconds, the method does not take into account the attitude and range dependent radar cross section of the interceptor. The direct collocation method is able to handle the nonlinearity of the radar cross section although this formulation will generally result in longer computation times. Additionally, the method is not guaranteed to converge to an optimal or even feasible solution.

Norsell has shown that the ground based radar problem can be solved with a more sophisticated aircraft model which includes varying speed and altitude.<sup>5</sup> The beam intercept is not limited to two dimensions and in many cases an altitude offset can aid in performing a VID. Future work will include an aircraft model with these capabilities.

For all of the approaches presented, the trajectory of the target aircraft was limited to trim flight in steady level or a constant turn rate. Future research could include a more sophisticated target which would take precautions to avoid a beam intercept. For example, the target could respond defensively or offensively when the interceptor violates the radar range constraint. It could also intelligently vary its heading so that its radar cone does not produce constant blind spots.

Radar blind spots can also be avoided by flying in formation. It is unlikely that the target aircraft will always fly alone. An ideal trajectory would include constraints considering the radar of all present aircraft. Additionally, the method should include which aircraft to pursue first.

The interceptor will most likely fly with support aircraft as well. The problem could include additional friendly aircraft which would be able to assist in performing visual identifications. The MILP approach can easily handle more aircraft. However, this might be difficult to include with the direct collocation approach.

## Acknowledgements

This research was funded under Draper Laboratory IR&D Project Number 12601.

## Disclaimer

The views expressed in this article are those of the author and do not reflect the official policy or position of the United States Air Force, Department of Defense, or the U.S. Government.

## References

- <sup>1</sup>Cry, Joe, "Radar Acronyms", <http://www.radomes.org/museum/scripts/jargon.cgi>.
- <sup>2</sup>Dever, Chris, Bernard Mettler, Eric Feron, Jovan Popovic, and Marc McConley, "Trajectory Interpolation for Parameterized Maneuvering and Flexible Motion Planning of Autonomous Vehicles", *Proceedings of AIAA Guidance, Navigation, and Control Conference and Exhibit*, Providence, RI, August 2004.
- <sup>3</sup>Hargraves, C.R., and S.W. Paris, "Direct Trajectory Optimization Using Nonlinear Programming and Collocation", *AIAA Journal of Guidance*, Vol.10, No.4, 1987, pp. 338-342.
- <sup>4</sup>Lambeth, B., *The Transformation of American Air Power*, Cornell University Press, Ithaca 2000, pp. 92-95.
- <sup>5</sup>Norsell, Martin, "Radar Cross Section Constraints in Flight Path Optimization", *Proceedings of 41st Aerospace Sciences Meeting and Exhibit*, Reno, NV, January 2003.
- <sup>6</sup>Repp, D., "History of 641<sup>st</sup> AC&W Squadron", <http://www.pinetreeline.org/other/other19/other19r.html>.
- <sup>7</sup>Richards, Arthur, and Jonathan P. How, "Aircraft Trajectory Planning with Collision Avoidance Using Mixed Integer Linear Programming", *Proceedings of the American Control Conference*, Anchorage, AK, May, 2002.
- <sup>8</sup>Richards, Arthur, Yoshiaki Kuwata, and Jonathan How, "Experimental Demonstrations of Real-time MILP Control", *Proceedings of the AIAA Guidance, Navigation, and Control Conference and Exhibit*, Providence, RI, August, 2004.
- <sup>9</sup>William, Lewis, "UCAV the Next Generation Air-Superiority Fighter?" Master dissertation, Air University, School of Advanced Airpower Studies, June 2002.
- <sup>10</sup>*Xpress-MP Essentials User's Guide*, Dash Optimization, 2002.